Fluorescence Energy Transfer as a Probe for Tetraplex Formation: The i-Motif

Jean-Louis Mergny*

Laboratoire de Biophysique, Muséum National d'Histoire Naturelle, INSERM U 201, CNRS URA 481, 43 rue Cuvier, 75005 Paris, France

Received September 14, 1998; Revised Manuscript Received December 4, 1998

ABSTRACT: The secondary structure of cytosine-rich oligodeoxynucleotides has been investigated with fluorescent probes. Intramolecular folding of an oligonucleotide into an i-DNA motif led to fluorescence excitation energy transfer between a donor (fluorescein) and an acceptor (tetramethylrhodamine) covalently attached to the 5′ and 3′ ends of the DNA, respectively, provided that a suitable linker was chosen. The conjugation of the dyes to the oligonucleotide had an influence on the thermodynamics of i-motif formation as well as on the kinetics of folding. Intramolecular folding was demonstrated from the concentration independence of FRET over a wide concentration range. Folding of the oligonucleotide was confirmed by UV absorption melting experiments. The folding of the i-motif could be followed at concentrations as low as 50 pM. Fluorescence energy transfer can thus be used to reveal the formation of multistranded DNA structures.

Fluorescence excitation energy transfer (FRET)[1] is a dipole−dipole resonance interaction between two "close" molecules, where one molecule, called the "donor", transfers its excitation energy to the other, called the "acceptor". FRET has provided valuable information about the structure of various biologically relevant molecules, including nucleic acids (*1*−*10*), because of its distance and orientation dependence (*11*). This study was undertaken to determine the potential use of derivatized oligonucleotides as probes of a tetraplex nucleic acid structure with the technique of fluorescence energy transfer.

It is well-known that cytosine-rich oligodeoxynucleotides or polynucleotides may adopt a non-B structure at acidic pH. The formation of C·C$^+$ base pairs was originally reported 30 years ago in crystals of acetylcytosine (*12*) and later in polydeoxy- or polyribonucleotides (*13*−*15*). The proposed hemiprotonated base pair is shown in Figure 1 (upper part). Solution studies of polydeoxycytidylic acid have pointed to the importance of hemiprotonation. The results showed that DNA sequences containing a significant stretch of cytosines could adopt complex pH-dependent conformations. Recently, the structure and stoichiometry of the complex formed by the hexamer d(T**CCCCC**) has been described (*16*). This so-called i-motif is a tetramer of equivalent strands, which exhibits the novel feature of intercalated C·C$^+$ base pairs of two parallel-stranded duplexes. Individual parallel-stranded duplexes are right-handed and underwound, and the two duplexes are "zipped together" in an antiparallel fashion (Figure 1, upper part). Crystallographic data for the d(**C-CCC**) and d(**CCC**T) oligodeoxynucleotides confirmed this structure (*17*, *18*). The molecule is flat with two very wide

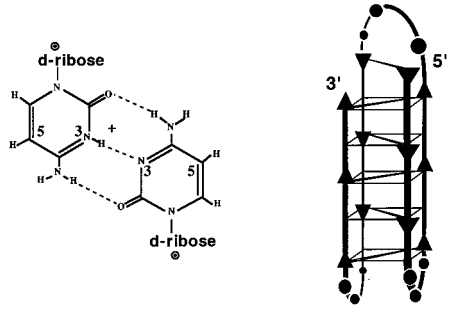

Oligonucleotide name	Sequence (5' → 3')
21	CCCTAACCCTAACCCTAACCC
F21	fluo- CCCTAACCCTAACCCTAACCC
21T	CCCTAACCCTAACCCTAACCC-tamra
F21T	fluo- CCCTAACCCTAACCCTAACCC-tamra
23	**TT**CCCTAACCCTAACCCTAACCC
F23	fluo- **TT**CCCTAACCCTAACCCTAACCC
23T	**TT**CCCTAACCCTAACCCTAACCC-tamra
F23T	fluo- **TT**CCCTAACCCTAACCCTAACCC-tamra
F23T2	fluo- CCCTAACCCTAACCCTAACCC **TA**-tamra
26	**TTTAA**CCCTAACCCTAACCCTAACCC
F26	fluo- **TTTAA**CCCTAACCCTAACCCTAACCC
26T	**TTTAA**CCCTAACCCTAACCCTAACCC-tamra
F26T	fluo- **TTTAA**CCCTAACCCTAACCCTAACCC-tamra
F-con-T	fluo- TTTTTTTTTTTTTTTTTTTTT-tamra
29	CCCCCTTTCCCCCTTTCCCCCTTTCCCCC
34	**TTTAA**CCCCCTTTCCCCCTTTCCCCCTTTCCCCC
F34T	fluo-**TTTAA**CCCCCTTTCCCCCTTTCCCCCTTTCCCCC-tamra

FIGURE 1: (Upper part) Hemiprotonated C·C$^+$ base pair (left) and schematic drawing of the i-motif (right). (Lower part) List of the oligonucleotides used in this study. Abbreviations used for the fluorescent oligonucleotide are indicated, with the following convention. The dye is written first if it is linked to the 5′ end of the oligonucleotide; when linked to the 3′ end, it is written last. fluo is fluorescein; tamra is tetramethylrhodamine.

* To whom correspondence should be addressed. Fax: (33-1) 40 79 37 05. E-mail: mergny@lovelace.infobiogen.fr.

[1] Abbreviations: FRET, fluorescence resonance energy transfer; Tamra, tetramethylrhodamine.

10.1021/bi982208r CCC: $18.00
Published on Web 01/12/1999

grooves and two very narrow grooves. The molecules twist in a right-handed manner, and the distance between the nearest base pairs is only 3.1 Å. Such a distance, which is shorter than that in B-DNA (3.4 Å), was reported for poly(dC) 30 years ago (*19*). A strand carrying four copies of the cytosine-rich telomeric repeat may form an intramolecular i-motif (*20*−*22*). Other biologically relevant sequences may also form this motif (*23*, *24*). In previous studies, we have determined the stability of the folded form(s) of different single-stranded oligodeoxy- or oligoribonucleotides (*25*, *26*). The data were collected using mostly UV absorbance melting experiments. We wanted to investigate whether fluorescence spectroscopy could provide useful information about the folding of a cytosine-rich oligonucleotide.

We describe some spectroscopic properties of derivatized oligodeoxynucleotides, where dyes such as fluorescein or rhodamine derivatives form the fluorescent part of the modified oligonucleotide. In the following experiments, we report that FRET can be used to probe the secondary structure of a cytosine-rich DNA fragment. We chose to analyze (1) a short oligonucleotide mimicking 3.5 repeats of the cytosine-rich strand of vertebrate telomeres with 4 repeats of 3 cytosines [this 21-base oligonucleotide was previously shown to form the i-motif, as demonstrated by two-dimensional NMR (*20*, *22*) and CD spectroscopy (*21*)] and (2) a longer oligonucleotide containing 4 repeats of 5 cytosines [this oligonucleotide forms a very stable i-motif (*25*)].

The primary sequences and names of the fluorescent oligonucleotides used therafter are given in the lower part of Figure 1.

EXPERIMENTAL PROCEDURES:

Oligonucleotides. All oligonucleotides were synthesized and purified by Eurogentec.

UV Absorption Studies. Unless otherwise specified, all experiments were performed in a 10 mM cacodylate buffer (pH 6.8) at an oligonucleotide strand concentration of 4 μM. Thermal denaturation profiles were obtained with a Kontron Uvikon 940 spectophotometer, using Quartz cuvettes with a 1 cm optical path length. The six-sample cell holders were thermostated by a circulating liquid (80% water/20% glycerol). The temperature of the liquid was controlled by an Haake water bath, and the temperature in one of the cells was measured by thermoresistance. The temperature of the bath was increased or decreased at a rate of 0.2 °C/min, thus allowing complete thermal equilibration of the six cuvettes.

Analysis of a Hysteresis. In many cases, we have observed that, at near-neutral pH, the thermal dissociation (heating) curves of the i-motif are largely shifted toward higher temperatures as compared to the association (cooling) curves (*22*, *25*). The hysteresis and the stability are strongly dependent on pH between pH 6.4 and 7.2. The kinetic behavior of the system has been analyzed at near-neutral pH to obtain the rate constants of association and dissociation from the hysteresis of the thermally induced association−dissociation reactions (*28*). Such a behavior, which is the result of slow association and dissociation kinetics, has already been described for triple helix formation (*27*). Quantitative analysis of the kinetic parameters of i-motif formation, based on the results of Rougée et al., with few modifications, will be presented elsewhere.

Fluorescence Studies. All measurements were taken on a Spex Fluorolog DM1B instrument, using a bandwidth of 1.8 nm and 0.2 cm × 1 cm quartz cuvettes. For emission spectra, the excitation wavelength was set at the wavelength where absorption of the donor was maximal (492 nm) or chosen to minimize the extent of absorption of the acceptor (480 nm). For excitation spectra, the emission wavelength was 580 nm. Correction of the emission spectra for instrumental response was achieved by recording the spectra of sample and standards, and correcting for absorbance differences.

(a) Calculation of R_o. R_o is the critical Förster distance, at which the transfer efficiency E accounts for half of the deactivation processes of the donor (*11*). R_o was calculated as described in ref *5*. We used an average value of $^2/_3$ for the orientation factor κ^2 (assuming random orientation for the two dyes; depending on the relative orientation of the emission dipole of the donor and the excitation dipole of the acceptor, κ^2 can take any value between 0 and 4) and 1.33 for the refractive index n. As the covalent link between the chromophore and the oligonucleotide has an effect on its absorption and fluorescence properties, ϵ, the absorption coefficient of the acceptor, and Φ_D, the quantum yield of fluorescence of the donor, were calculated from the data obtained for the conjugated dyes. E is linked to R_o by the following formula:

$$E = \frac{R_o^{\,6}}{R_o^{\,6} + R^6} \qquad (1)$$

where R is the distance between the donor and acceptor. Due to the sixth-power dependence on R, E very quickly drops to zero when $R > R_o$.

(b) Determination of Transfer Efficiency E. E can usually be calculated from the quenching of the donor emission in the presence of the acceptor, provided that no other phenomenon perturbs the fluorescence of the donor. This quenching was monitored at a wavelength where the emission of the acceptor was negligible (515 nm for the fluorescein−tamra couple).

RESULTS

Fluorescence Properties of the Conjugated Dyes. The spectroscopic properties of fluorescein and tamra were affected by covalent linkage to the oligonucleotide. The maximum absorption and excitation wavelength for 21-mer−fluorescein was 492 nm, with an emission maximum at 512 nm, and a quantum yield (0.2) which was lower than that of free fluorescein. The oligonucleotide linked to tamra had maximum excitation (557 nm) and emission (581 nm) wavelengths very similar to those of the protein-conjugated dye (555 and 580 nm, according to Molecular Probes). Note that the molar extinction coefficient of fluorescein was decreased by 30% for fluorescein ($\epsilon = 3.6 \times 10^4\ M^{-1}\ cm^{-1}$) upon covalent linkage. Such a decrease has already been described for fluorescein conjugated to an oligonucleotide (*5*). The properties of the fluorescein-conjugated oligonucleotides were also strongly dependent on pH, and an important quenching was observed at pH <6.8. For these reasons, all measurements were performed in a pH 6.8 buffer, which was

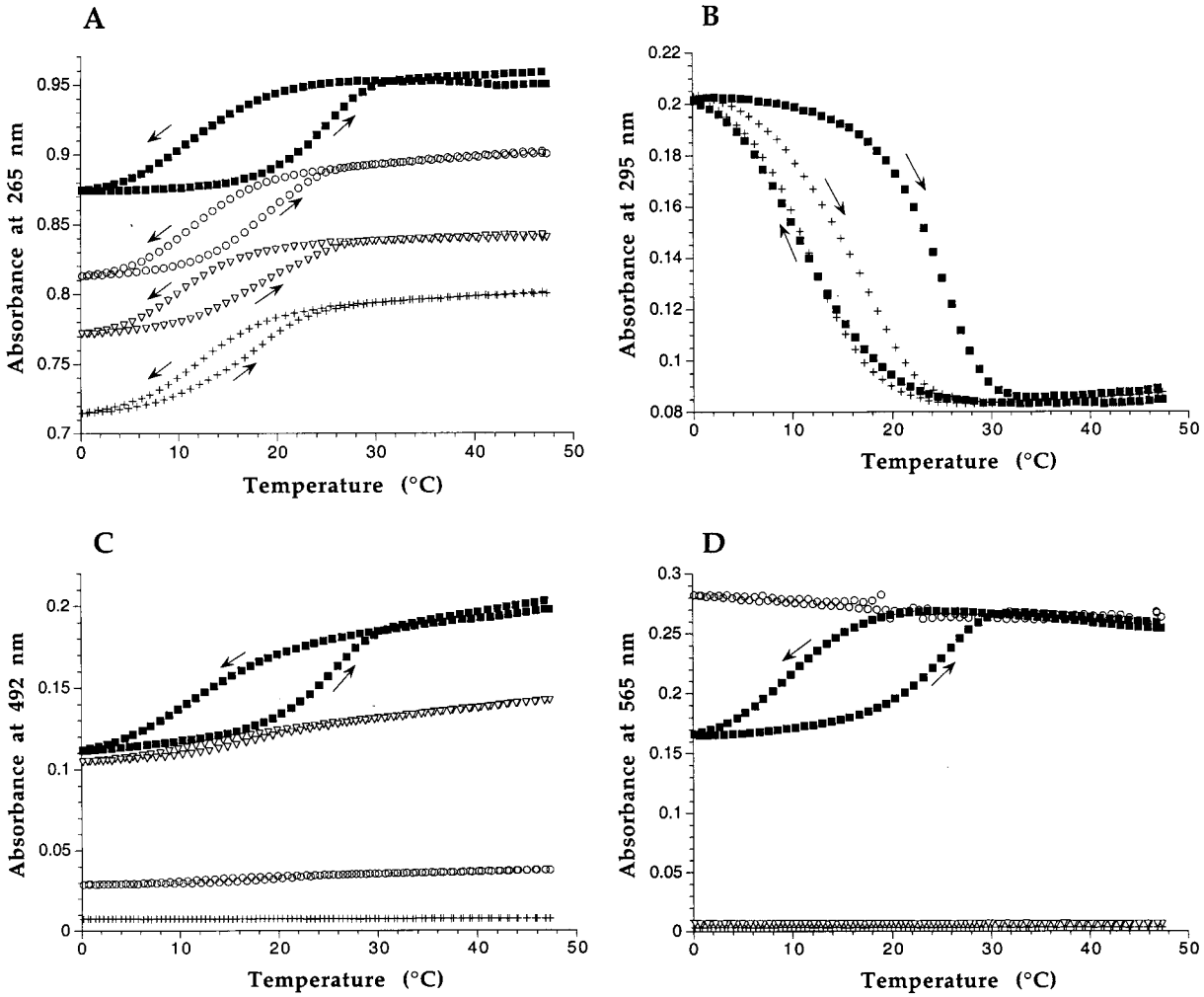

FIGURE 2: UV denaturation profiles of the 21-mer (+), F21 (▽), 21T (○), and F21T (■) in a pH 6.8, 10 mM cacodylate buffer (4 μM strand concentration). Directions of temperature changes are indicated by arrows. (A) Absorbance recorded at 265 nm, with 0.06, 0.12, and 0.18 OD offsets for F21, 21T, and F21T, respectively. (B) Absorbance recorded at 295 nm. Only the data for the 21-mer and F21T are presented in this part for clarity. (C) Absorbance recorded at 492 nm. (D) Absorbance recorded at 565 nm.

acidic enough to allow i-motif formation, without an overly important quenching of the fluorescence of the donor.

Excitation Energy Transfer Studies for 21-mers. In the unfolded form, little transfer is expected, as the average distance of the two chromophores should be larger than the Förster critical distance (calculated to be around 4.5 nm). Intramolecular folding should bring the chromophores into close enough proximity. Therefore, FRET should be a convenient method for monitoring the 3′ to 5′ end distance.

We first wanted to confirm that the covalent attachment of the dyes did not prevent i-motif formation. The "parent" oligonucleotide (21-mer) has been shown to fold into an i-motif structure by NMR spectroscopy (*22*), and UV melting experiments provided a good test for measuring the stability of the structure. Therefore, T_m measurements were taken for the 21, F21, 21T, and F21T oligomers at pH 6.8. As shown in Figure 2A, a hyperchromic shift was observed for all oligonucleotides. In all cases, the heating and cooling cycles could not be superimposed; the profile obtained when the temperature was increased was shifted to higher temperatures as compared to the profile observed when the temperature was decreased. This hysteresis phenomenon, which has been described for DNA triple helices (*27*), has been studied in the case of i-motif formation (*28*). This hysteresis is the consequence of slow kinetics of i-motif formation and dissociation at near-neutral pH. All transitions were pH-dependent, in agreement with i-motif formation (not shown).

The four oligonucleotides melted in the same temperature range, but their melting profiles were not perfectly superimposable, suggesting that the covalent attachment of one or two fluorescent dyes had a significant impact on the stability of the folded structure (Figure 2A). A larger hysteresis at 265 nm was present in the case of the F21T oligonucleotide, as a result of slower association−dissociation kinetics. Figure 2B is the melting profile at 295 nm for the 21 and F21T oligomers. As previously observed, dissociation of the i-motif induces a hypochromic shift at this wavelength, as a result of cytosine deprotonation (*25*). The hysteresis phenomenon was also more pronounced at 295 nm in the case of the F21T oligonucleotide, and the heating curve was significantly shifted toward higher temperatures. Therefore, the double substitution delays the dissociation of the i-motif and stabilizes the structure. Simple substitutions (F21 or 21T) had less effect on the stability, as compared to that of the nonfluorescent 21-mer.

Panels C and D of Figure 2 show the absorbance versus temperature profiles at two other wavelengths, in the visible region, close to the absorbance maxima for fluorescein (492

nm, Figure 2C) and tamra (565 nm, Figure 2D). The unsubstituted 21-mer does not absorb light in the visible region (+). The 21T shows a monotonic variation of absorbance at these two wavelengths (○). The absorbance of the F21 oligomer at 492 nm (▽, Figure 2C) is only slightly affected by i-motif formation. These weak variations are in sharp constrast with the large signals observed at 492 (Figure 2C) and 565 nm (Figure 2D) for the doubly substituted F21T oligomer. These absorbance measurements show that, upon i-motif formation, a significant hypochromism is observed for the tamra and fluorescein dyes, when they are brought into close proximity. No such hypochromism was obtained with the simply substituted oligomers, suggesting that this hypochromism is the result of direct tamra−fluorescein interaction, rather than the result of an interaction between the dye and the structure itself.

We then performed fluorescence measurements as a function of temperature for the F21 and F21T oligomers. As shown in Figure 3A, when excitation was set at 492 nm, a decrease of fluorescence emission at 515 nm was observed at low temperatures for the F21 oligomer (▽). The shape of this fluorescence versus temperature profile was very similar to that of the absorbance at 265 nm versus temperature profile (Figure 2A, ▽). i-motif formation induces a 50% quenching of fluorescence. The temperature dependence of the F21T oligomer emission at 515 nm was even more pronounced, and a 96% quenching of fluorescence was observed at 0 °C, as compared to that at 40 °C. This quenching was in part the result of a decrease in fluorescein absorbance (Figure 2C, ■); however, the decrease in fluorescein emission (96%) cannot be solely explained by the decrease in the absorption coefficient (30%). Therefore, both fluorescein absorbance and fluorescence properties are altered in the presence of tamra.

On the basis of fluorescein emission only, one cannot conclude that fluorescence energy transfer is observed at low temperatures for the F21T oligomer. The analysis of the acceptor emission at 580 nm revealed that, upon excitation at 492 nm, no sensitized emission of the acceptor was observed. On the contrary, a significant decrease in tamra emission was observed (Figure 3A, □). Therefore, although one cannot completely exclude the possibility that FRET occurs in this system, it is not the major mechanism that explains the quenching of the fluorescence of the donor. Rather, as suggested by the absorbance measurements (panels C and D of Figure 2), direct interaction between the two dyes may occur, and prevent fluorescence emission.

Identical measurements were performed with the FconT oligonucleotide, with fluorescein and tamra conjugated at the 5′ and 3′ ends, respectively. Monotonic variations of fluorescein and tamra emission were observed in the temperature range of 0−80 °C, and no quenching of the emission of fluorescein was detected, in agreement with an unfolded structure at all temperatures (not shown).

Excitation Energy Transfer Studies for 23-mers. In the case of the 21-mers, fluorescein and tamra were directly attached to the 5′ and 3′ ends of the i-motif, respectively. Folding of the oligonucleotide should lead to the juxtaposition of the two dyes. For this reason, we designed longer oligonucleotides, having two extra bases at the 5′ (F23T) and 3′ (F23T 2) ends, to increase the distance between the two chromophores and prevent direct physical interaction.

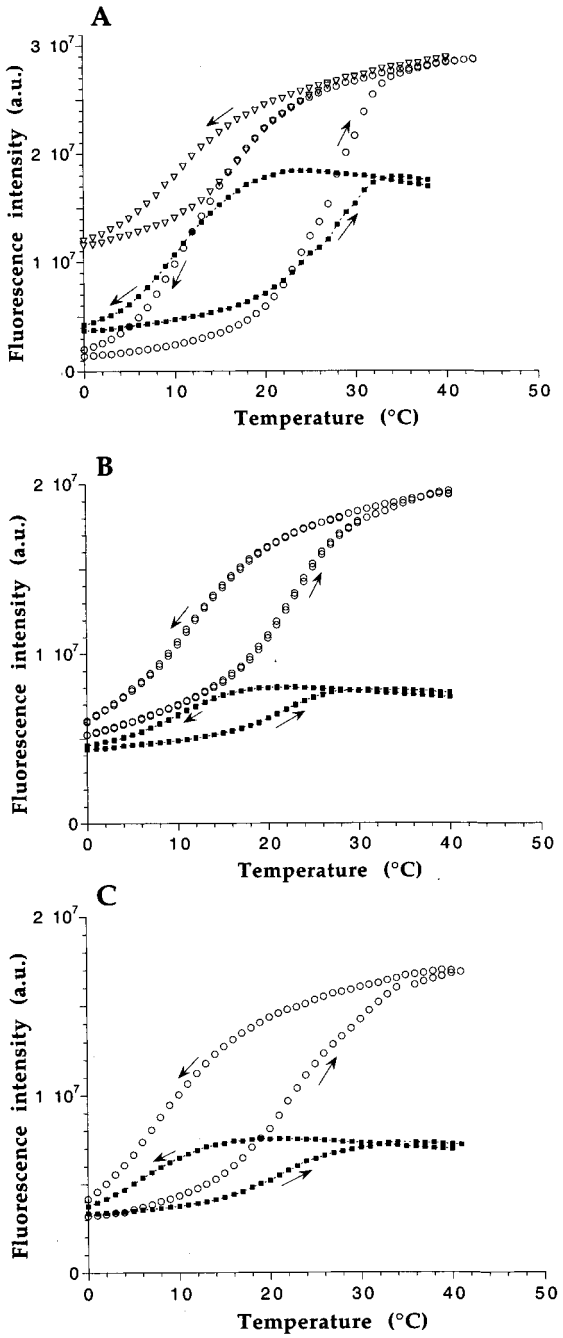

FIGURE 3: Fluorescence vs temperature measurements in a pH 6.8, 10 mM cacodylate buffer (0.2 μM strand concentration). Excitation was set at 492 nm. The temperature of the bath was increased or decreased at a rate of 0.25 °C/min. Directions of temperature changes are indicated by arrows: (A) F21T (515 nm, ○; 580 nm, ■) and F21 (515 nm, ▽), (B) F23T (515 nm, ○; 580 nm, ■), and (C) F23T2 (515 nm, ○; 580 nm, ■).

Absorbance measurements at four different wavelengths (265, 295, 492, and 565 nm; not shown) gave results similar to the melting curves presented in Figure 2 for the 21-mers; the F23T oligomer has a different melting profile at 265 nm than the 23-mer and F23 and 23T oligomers. As for the F21T in panels C and D of Figure 2, the absorbance at 492 and 565 nm of the F23T decreased at low temperatures (not shown). Fluorescence versus temperature measurements were taken by simultaneously recording emission at 515 and 580 nm for the F23T (Figure 3B) and F23T2 (Figure 3C) oligomers. In both cases, quenching of donor and acceptor

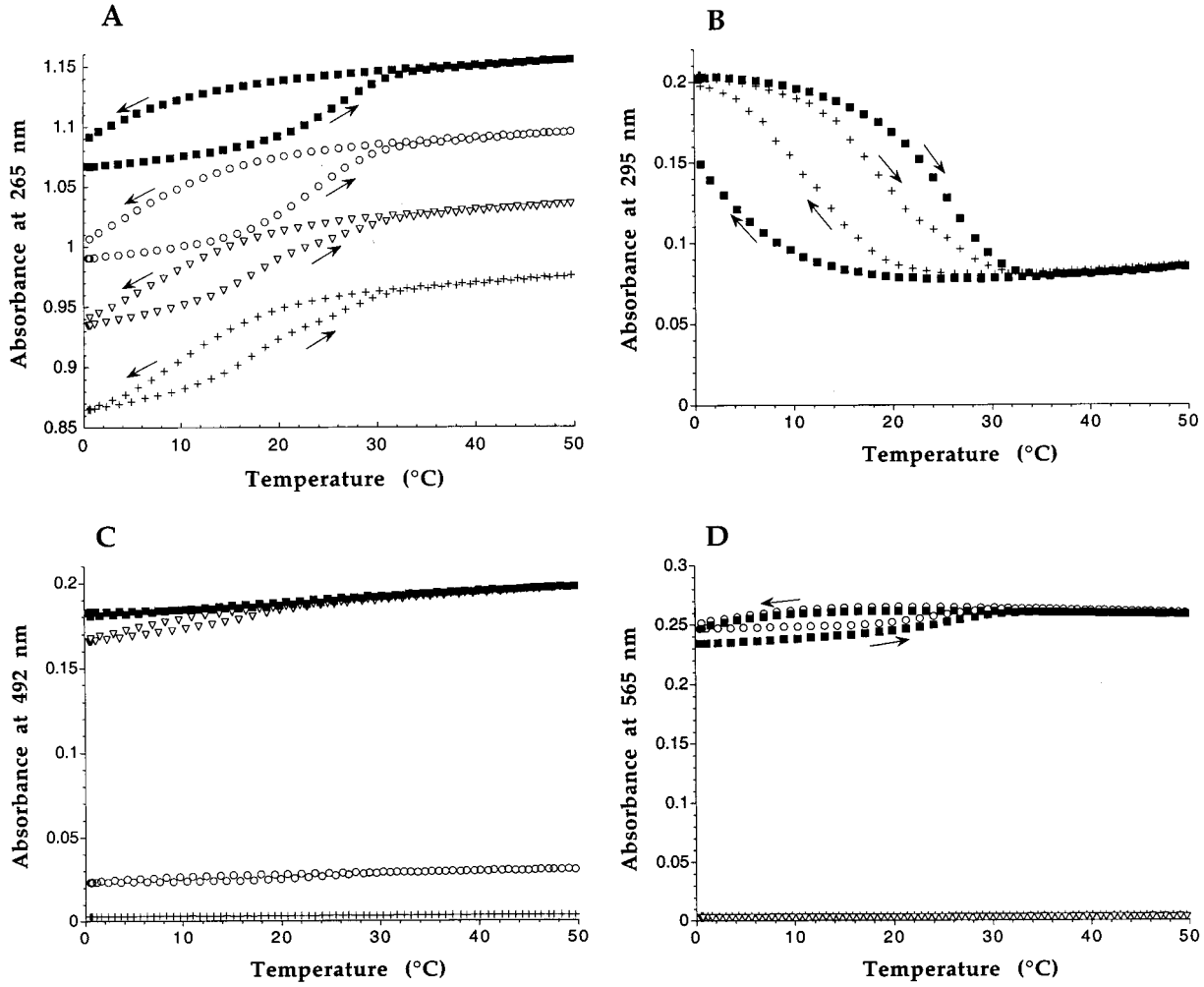

FIGURE 4: UV denaturation profiles of the 26-mer (+), F26 (▽), 26T (○), and F26T (■) in a pH 6.8, 10 mM cacodylate buffer (4.2 μM strand concentration). Directions of temperature changes are indicated by arrows. (A) Absorbance recorded at 265 nm, with 0.06, 0.12, and 0.18 OD offsets for F26, 26T, and F26T, respectively. (B) Absorbance recorded at 295 nm. Only the data for the 26-mer and F26T are presented in this part for clarity. (C) Absorbance recorded at 492 nm. (D) Absorbance recorded at 565 nm.

emission was observed at low temperatures, and the shapes of the fluorescence melting curves were superimposed with the UV absorbance melting curves. Therefore, in both cases, i-motif formation led to direct interaction between fluorescein and tamra, and no FRET could be detected. In conclusion, the addition of two extra bases at the 5′ or 3′ end was not sufficient to completely prevent a direct interaction of the two dyes. Nevertheless, the quenching of fluorescein emission was less pronounced in the case of the F23T and F23T2 oligomers (70 and 80%, respectively) than in the case of the F21T oligonucleotide (96%).

Excitation Energy Transfer Studies for 26-mers. For this reason, we designed even longer oligonucleotides, having five extra bases at the 5′ end, to further increase the distance between the two chromophores and prevent direct physical interaction.

Absorbance measurements at four different wavelengths (265, 295, 492, and 565 nm) are presented in Figure 4 for the 26-mer (+) and F26 (▽), 26T (○), and F26T (■) oligonucleotides. Several conclusions can be reached on the basis of these UV melting curves.

(i) The unsubstituted 26-mer has a slightly different profile than the parent 21-mer (compare Figure 4A, crosses, with Figure 2A, crosses). In other words, the addition of five extra bases at the 5′ end of the sequence has an impact on the formation of the i-motif.

(ii) Figure 4A shows that the profiles of 26 and F26 are identical, but differ from the profiles of the 26T and F26T oligomers. No difference was observed between the 26T and F26T oligomers. In other words, the addition of a fluorescein at the 5′ end of the oligomer has little effect on i-motif formation, whereas a tamra at the 3′ end leads to a larger hysteresis, showing that the kinetics of association and dissociation are slowed by this 3′ end modification.

(iii) Figure 4B confirms the data recorded at 265 nm; at 295 nm, an inverted transition is obtained for both the 26-mer and the F26T oligomer, and the hysteresis is more pronounced in the case of the F26T oligomer.

(iv) Figure 4C shows that the absorbance of the fluorescein dye is not affected by the formation of the i-motif, even in the presence of the tamra dye; a monotonic variation of absorbance is obtained for the F26 and F26T oligomers.

(v) In contrast, the absorbance of the tamra dye is slightly affected by the formation of the i-motif, in the presence or in absence of the fluorescein dye; a small variation of absorbance is observed at 565 nm for the 26T and F26T oligomers (Figure 4D).

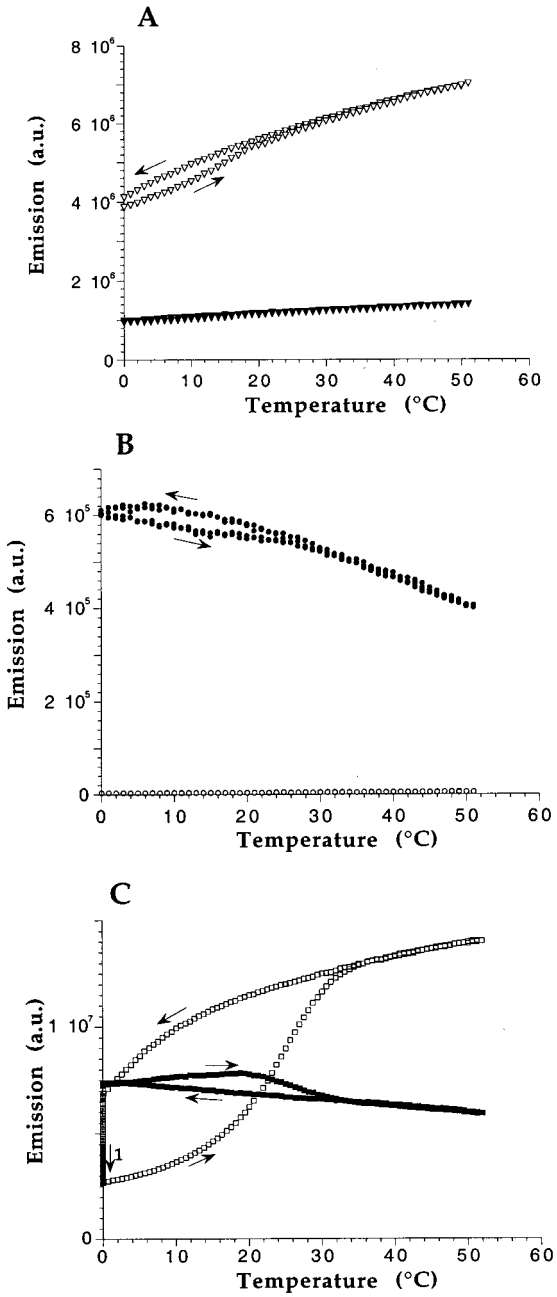

FIGURE 5: Fluorescence vs temperature measurements in a pH 6.8, 10 mM cacodylate buffer (0.2 μM strand concentration). Excitation was set at 492 nm. Emission was recorded at 515 (white symbols) or 580 nm (black symbols). The temperature of the bath was increased or decreased at a rate of 0.25 °C/min. Directions of temperature changes are indicated by arrows: (A) F26 (515 nm, ▽; 580 nm, ▼), (B) 26T (515 nm, ○; 580 nm, ●), and (C) F26T (515 nm, □; 580 nm, ■).

(vi) These experiments show that the tamra dye, but not the fluorescein dye, has a significant effect on the formation of the i-motif. Contrary to what was shown for the 21-mers in Figure 2, no interaction between the fluorescein and tamra dyes was detected for the doubly substituted F26T oligonucleotide.

Fluorescence versus temperature measurements were taken by simultaneously recording emission at 515 and 580 nm for the F26 (Figure 5A), 26T (Figure 5B), and F26T (Figure 5C) oligomers. In the case of the F26 and 26T oligomers, no large variation of fluorescence was observed. A limited quenching of fluorescein emission was detected at low

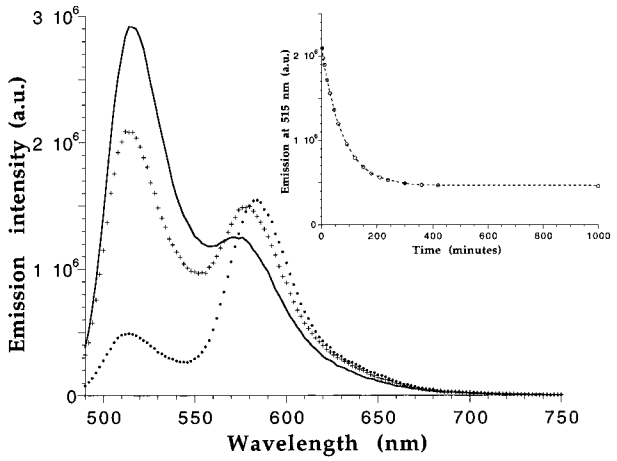

FIGURE 6: Fluorescence emission spectra of F26T (0.2 μM strand concentration, λ_{exc} = 480 nm) in a pH 6.8, 10 mM cacodylate buffer: (solid line) at 37 °C, (+) after a 2 min incubation at 0 °C, and (●) after a 5 h incubation at 0 °C. (Inset) Time dependence of the fluorescence emission of F26T. The sample was denatured at high temperatures and then quickly cooled to 0 °C. Fluorescence measurements (excitation at 492 nm and emission at 515 nm) were then performed at different times.

temperatures for the F26 oligonucleotide (Figure 5A). This minor variation is in sharp contrast with the large hysteresis presented in Figure 5C for the F26T oligomer. A maximum quenching of 80% at 0 °C was detected. However, a 5 h preincubation at 0 °C was required to maximize the quenching, and a slow decrease in emission at 515 nm was detected during this period (arrow 1 in Figure 5C). This result is in good agreement with the UV melting profile (Figure 4A) showing that, even after slow cooling to 0 °C, re-formation of the structure was not completed immediately.

To analyze the kinetics of i-motif formation at 0 °C, the F26T oligomer was heat denatured and kept at 37 °C. Its emission spectrum is shown in Figure 6 (solid line). The sample was then quickly equilibrated at 0 °C, and emission spectra were recorded at different time intervals. Figure 6 presents the emission spectrum after 2 min (+) at 0 °C and after 5 h at 0 °C (●). The quantitation of the emission signal at 515 nm versus time is presented in Figure 6 (inset). From these data, one may observed that at least 5 h is required to obtain near-complete formation at 0 °C. The curve could well be fitted with a monoexponential decay, with a half-life of 70 min, in good agreement with a first-order kinetic reaction, as expected for intramolecular folding.

From the shape of the emission curve presented in Figure 6A, one may observe that the emission signal at 580 nm (in the acceptor emission range) is not strongly increased upon i-motif formation. To demonstrate that FRET effectively occurred between the donor and the acceptor, we recorded the emission (Figure 7A) and excitation (Figure 7B) spectra of the F26 (▽), 26T (○), and F26T (■) oligomers. The analysis of the emission spectra, after excitation at 480 nm, shows that the emission at 515 nm of F26T is strongly quenched, as compared to that of F26. In other words, the addition of a tamra group at the 3′ end of the 26-mer strongly quenches the emission of fluorescein. At longer wavelengths (around 580 nm), a relatively high emission level is observed for F26T. This peak may be explained only in part by a direct excitation at 480 nm of the tamra dye (see the emission of 26T for comparison). The analysis of the excitation spectra

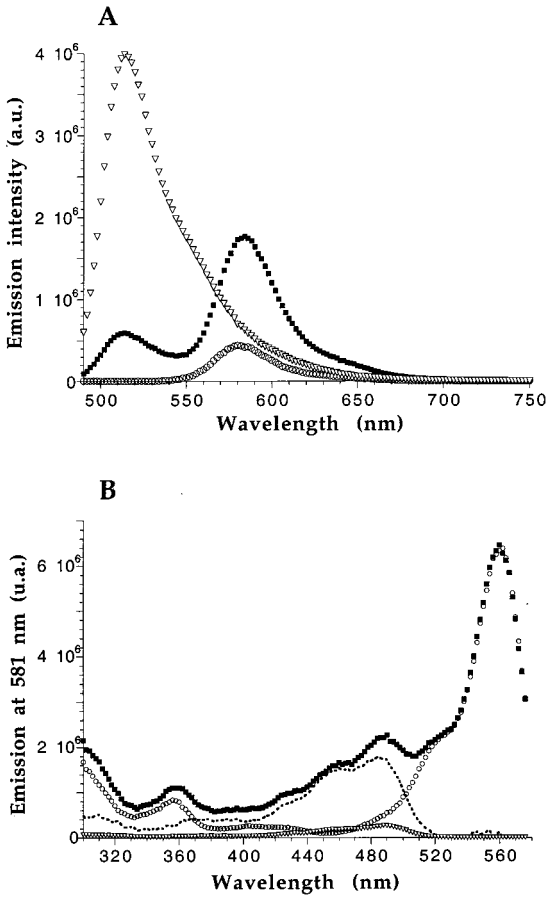

FIGURE 7: Fluorescence spectra of F26 (▽), 26T (○), and F26T (■) with a 0.2 μM strand concentration in a pH 6.8, 10 mM cacodylate buffer at 0 °C. The samples were equilibrated at 0 °C for 72 h before the measurements. (A) Fluorescence emission spectra (excitation set at 480 nm). (B) Fluorescence excitation spectra (emission set at 580 nm). The dotted line depicts the subtraction of 26T from F26T excitation spectra.

(emission recorded at 580 nm) confirms that this enhanced emission is the result of the excitation of the fluorescein dye [compare the excitation spectra of F26T (■) with those of 26T (○)]. In other words, this emission peak at 580 nm is in large part the result of FRET from fluorescein to tamra.

Excitation Energy Transfer Studies for 34-mers. The stability of the i-motif formed by the telomeric sequence (CCCTAA repeats) is, as previously observed, marginal at near-neutral pH (*22*). We thus wanted to investigate by FRET the formation of a more stable i-motif. Increasing the length of the cytosine repeats stabilizes the structure (*25*). Therefore, we studied the folding of a 29-mer, containing 4 repeats of 5 cytosines. Its sequence is presented in Figure 1. For FRET studies, on the basis of the data obtained with the 26-mers, we designed a derivative of the 29-mer sequence, with an identical 5′-TTTAA five-base tail. The thermal stabilities of the 29- and 34-mers and F34T oligomer are presented in Figure 8A. As expected, the melting of the 29-mer (◇) occurred at higher temperatures than the melting of the telomeric repeat oligonucleotide (21-mer, shown in Figure 2A). A large hysteresis was observed, and an apparent melting temperature of 43 °C was obtained upon heating, as compared to 32 °C upon cooling. The addition of a 5′ tail increased the hysteresis (Figure 8A, +). Melting occurred at 45 °C when the sample was heated, but re-formation of the folded structure by cooling was even more delayed

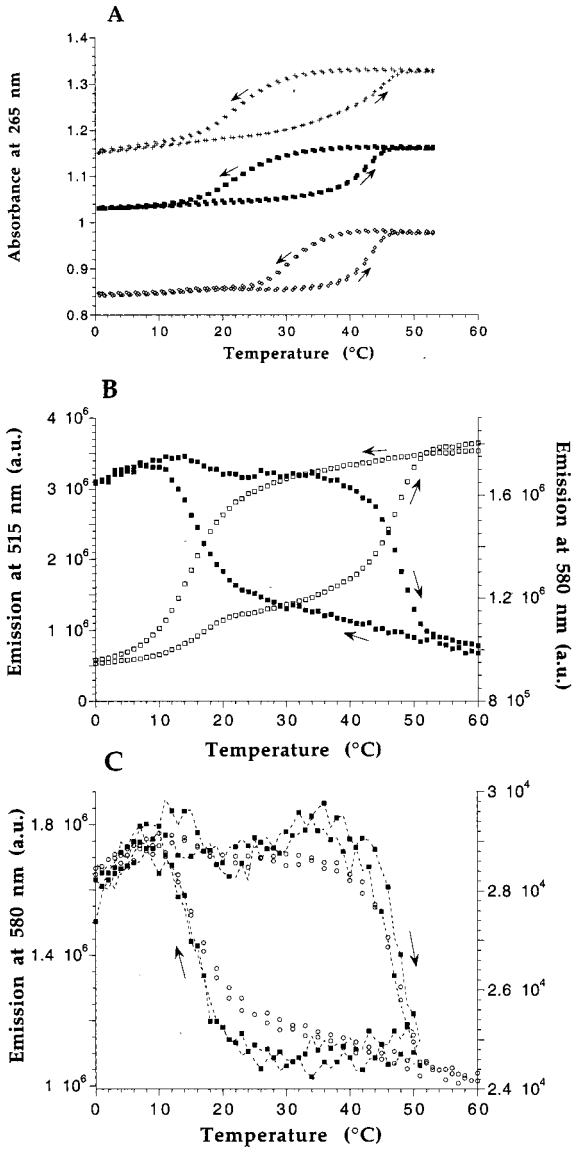

FIGURE 8: (A) UV denaturation profiles of the 29-mer (◇), the 34-mer (+), and F34T (■) in a pH 6.8, 10 mM cacodylate buffer (2.2 μM strand concentration). (B) Fluorescence vs temperature measurements of F34T in a pH 6.8, 10 mM cacodylate buffer (0.2 μM strand concentration). Excitation was set at 492 nm. Emission was recorded at 515 (□) or 580 nm (■). The temperature of the bath was increased or decreased at a rate of 0.25 °C/min. (C) Concentration dependence of the fluorescence vs temperature measurements of F34T (0.2 μM, ○; 50 pM, ■). Excitation was set at 492 nm. Emission was recorded at 580 nm. The temperature of the bath was increased or decreased at a rate of 0.25 °C/min. Larger emission and excitation slits were used for the diluted sample (9.2 nm) than for the 0.2 μM sample (1.8 nm). All these measurements were performed in a pH 6.8, 10 mM cacodylate buffer. Directions of temperature changes are indicated by arrows.

(apparent T_m of 23 °C). In this case, the T_m determined from the heating experiment differs from the T_m deduced from the cooling process by more than 20 °C! Two successive heating and cooling processes are presented in Figure 8A, showing that this phenomenon is perfectly reproducible. In this case, the addition of both dyes has little effect on the stability of the structure [compare 34-mer (+) and F34T (■) in Figure 8A].

Fluorescence melting experiments were then performed with the F34T oligonucleotide, exactly as described for F21T (Figure 3A), F23T (Figure 3B), F23T2 (Figure 3C), and

F26T (Figure 5C). The results are presented in Figure 8B. An important quenching (85%) of fluorescein emission at 515 nm was observed at low temperatures. This is in contrast with the sensitized increased emission level at 580 nm. In this case, formation of the i-motif led to an 80% increase in emission at 580 nm. As previously observed for the 26-mers, the fluorescence signals follow the absorbance melting curves, and a large hysteresis is obtained. Full quenching of the donor is achieved in a matter of minutes (not shown). This association process, which is faster than that for the 26-mer, is the result of the greater thermal stability of the 34-mer and the very strongly negative activation energies of association. In other words, k_{on} strongly increases when the temperature decreases (*28*), in a manner analogous to the nucleation-zipping model proposed for double- and triple-stranded nucleic acids.

All these studies confirm that, provided that two chromophores are attached to an i-motif forming oligonucleotide, FRET may be used to monitor the formation of the tetraplex. All fluorescent measurements were taken at 0.2 μM, as compared to a strand concentration of 4 or 4.2 μM in the case of absorbance measurements. We tested further the sensitivity of this method; Figure 8C presents the fluorescence emission signal at 580 nm recorded for F34T at two different concentrations: 0.2 μM (○, emission intensity shown on the left scale) and 50 pM (■, emission intensity shown on the right scale). Melting and cooling profiles were very similar. Two heating and cooling cycles are presented in each case, showing that the hysteresis phenomenon was clearly reproducible. Therefore, folding of F34T into an i-DNA motif could be detected at concentrations as low as 5×10^{-11} M with this method.

DISCUSSION

FRET versus Static Quenching. Donor−acceptor interactions other than dipole−dipole should usually be avoided. These interactions usually occur when the two molecules are brought into very close proximity (a few angstroms). Folding of the 21-mer, where the fluorescein and tamra dyes are directly linked to the terminal 5′ and 3′ cytosines, led to a strong quenching of the donor fluorescence. It was possible to prevent such a close contact, for example, by inserting a few bases between the two dyes. Two bases were not sufficient, but a 5′ spacer of five bases prevents undesired contact between the two dyes. When the resulting 26-mer folded, FRET was obtained between fluorescein and tamra, as shown by the quenching of fluorescein emission and the sensitized tamra emission.

It should be noted that the quenching of the donor fluorescence was less pronounced than in the case of the 21-mer. Therefore, the fluorescence variation of the fluorescein group of the F21T oligomer is a very sensitive way of monitoring the folding of this oligonucleotide; a 25-fold increase of fluorescence is observed upon i-motif dissociation. Nevertheless, the absence of a concomitant sensitized emission could lead to wrong conclusions; fluorescein emission is very sensitive to experimental conditions, such as pH, and a large variation of its emission might result from a different phenomenon (i.e., change of the local environment) than the intramolecular folding of the oligomer. In the case of the F26T oligomer, the enhanced emission of the tamra species is further proof of FRET.

Quantitative Measurement of Fluorescence Energy Transfer. As shown in this study, covalent attachement of the dye has an impact on the fluorescence properties of the dyes, especially fluorescein. It is also noteworthy than the extinction coefficient and relative quantum yield of covalently bound fluorescein are themselves dependent on the state of the oligonucleotide (i.e., folded or unfolded) especially when it is directly attached to the i-motif, without any linker bases in between. Therefore, the R_o distance between fluorescein and tamra is slightly different in the case of folded and unfolded oligomers. The fluorescence properties of these dyes, and especially fluorescein, are also strongly dependent on experimental conditions, which may explain the apparent discrepancies between the R_o values reported for this donor−acceptor pair (from 3.5 to 5.2 nm).

Another important factor concerning FRET is its distance and orientation dependence. The orientation factor $\langle \kappa^2 \rangle$ can be precisely determined in two extreme cases: when the orientations of the two molecules have an isotropic distribution or if their position is fixed and known. For the experiments described in this study, all fluorophores had a limited freedom, and the distribution of their orientation factors was certainly not isotropic, mainly because the target strand sterically prevents some of the orientations, and the fluorophores closely interact with the target sequence. This leads to an error in the orientation factor, which is often assumed to be equal to $^2/_3$ (isotropic distribution) for all R_o determinations, but could well take any value between 0 and 4. Two structures could be compared, on the basis of the transfer efficiency, but the geometry and the eventual folding of the nucleic acid linker between the donor and the acceptor also have an influence on the average distance between the two molecules. Thus, both the distance and orientation of the two molecules might be affected. Pertinent conclusions can only be drawn if the fluorophores experience complete motional freedom or immobility.

Influence of the Reporter Group on the Stability of the i-Motif. This study illustrates one of the major drawbacks of using fluorescence spectroscopy to monitor the stability of a nucleic acid structure. As nucleic acids are virtually nonfluorescent, attachement of a reporter dye(s) is needed to monitor the fluorescence of the oligomer. The structural effect of such a modification is usually neglected. This is not the case in the formation of the i-motif for two main reasons. (i) The oligonucleotides are rather small, and therefore, the attachment of a dye has a significant impact on the molecular weight, charge, flexibility, and hydrophobicity of the molecule. (ii) The stability of the i-motif at neutral pH is relatively weak, and a stabilizing effect obtained in the presence of a terminal dye will be easily detected. Finally, the bulkiness of the reporter dyes interferes with the folding and unfolding of the i-motif. As a result, the dissociation and association constants of the fluorescent oligonucleotides are lower than the calculated values obtained with an unmodified oligomer with an identical sequence.

Why Should FRET Be Used? All the experiments described above require a doubly labeled oligonucleotide, with a donor group at one end and an acceptor group at the other end. The synthesis and purification of such an oligonucleotide is rather long and costly, compared to that of an unmodified oligomer. The yields of labeling for both dyes must be high, and a good separation of the fluorescent derivatives is not

always straightforward. As a result, minute amounts of pure, doubly substituted oligomers are often obtained. Finally, the labeling may have a significant impact on the properties of the oligonucleotide.

There are justifications for the FRET approach that balance the disadvantages. (i) The technique is extremely sensitive, allowing detection of the phenomenon at a strand concentration of 5×10^{-11} M. Therefore, low yields of synthesis are not a major problem. (ii) The dynamic response of most spectrofluorimeters is linear over a wide concentration range (typically 5 orders of magnitude). Association phenomena may thus be followed at different concentrations, allowing the determination of thermodynamic parameters. In our case, intramolecular folding led to a concentration-independent behavior demonstrated between strand concentrations between 5×10^{-11} and 2×10^{-7} M. (iii) The technique may be used to follow the folding of a fluorescent oligonucleotide, even in the presence of a large excess of unlabeled polymers. Thus, FRET may be used in cultured cells (*9*); the degradation or the structure of an oligonucleotide has been successfully assessed using this technique.

In conclusion, FRET is a valuable method for investigating the secondary structure of an oligonucleotide. We are currently exploring the possibility of analyzing the structure of an i-motif oligonucleotide in the presence of various ligands or proteins.

ACKNOWLEDGMENT

I thank C. Hélène, T. Garestier, M. Lemaître, L. Lacroix, and H. Liénard for helpful discussions.

REFERENCES

1. Murchie, A. I. H., Clegg, R. M., Kitzing, E., Duckett, D. R., Diekmann, S., and Lilley, D. M. J. (1989) *Nature 341*, 763−766.
2. Clegg, R. M., Murchie, A. I. H., Zechel, A., Carlberg, C., Diekmann, S., and Lilley, D. M. J. (1992) *Biochemistry 31*, 4846−4856.
3. Clegg, R. M., Murchie, A. I. H., Zechel, A., and Lilley, D. M. J. (1993) *Proc. Natl. Acad. Sci. U.S.A. 90*, 2994−2998.
4. Eis, P. S., and Millar, D. P. (1993) *Biochemistry 32*, 13852−13860.
5. Mergny, J. L., Boutorine, A. S., Garestier, T., Belloc, F., Rougée, M., Bulychev, N. V., Koshkin, A. A., Bourson, J., Lebedev, A. V., Valeur, B., Thuong, N. T., and Hélène, C. (1994) *Nucleic Acids Res. 22*, 920−928.
6. Gohlke, C., Murchie, A. I. H., Lilley, D. M. J., and Clegg, R. M. (1994) *Proc. Natl. Acad. Sci. U.S.A. 91*, 11660−11664.
7. Mergny, J. L., Garestier, T., Rougée, M., Lebedev, A. V., Chassignol, M., Thuong, N. T., and Hélène, C. (1994) *Biochemistry 33*, 15321−15328.
8. Yang, M. S., Ghosh, S. S., and Millar, D. P. (1994) *Biochemistry 33*, 15329−15337.
9. Sixou, S., Szoka, F. C., Green, G. A., Giusti, B., Zon, G., and Chin, D. J. (1994) *Nucleic Acids Res. 22*, 662−668.
10. Vámosi, G., Gohlke, C., Murchie, A. I. H., Lilley, D. M. J., and Clegg, R. M. (1993) http://www.mpibpc.gwdg.de/abteilungen/060/people/clegg/poster/.
11. Förster, T. (1948) *Ann. Phys. 2*, 55−75.
12. Marsh, R. E., Bierstedt, R., and Eichhorn, E. L. (1962) *Acta Crystallogr. 15*, 310−316.
13. Akinrimisi, E. O., Sander, C., and Tso, P. O. P. (1963) *Biochemistry 2*, 340−344.
14. Langridge, R., and Rich, A. (1963) *Nature 198*, 725−728.
15. Inman, R. B. (1964) *J. Mol. Biol. 9*, 624−637.
16. Gehring, K., Leroy, J. L., and Guéron, M. (1993) *Nature 363*, 561−565.
17. Chen, L., Cai, L., Zhang, X. H., and Rich, A. (1994) *Biochemistry 33*, 13540−13546.
18. Kang, C. H., Berger, I., Lockshin, C., Radliff, R., Moyzis, R., and Rich, A. (1994) *Proc. Natl. Acad. Sci. U.S.A. 91*, 11636−11640.
19. Hartman, K. A., and Rich, A. (1965) *J. Am. Chem. Soc. 87*, 2033.
20. Ahmed, S., Kintanar, A., and Henderson, E. (1994) *Nat. Struct. Biol. 1*, 83−88.
21. Manzini, G., Yathindra, N., and Xodo, L. E. (1994) *Nucleic Acids Res. 22*, 4634−4640.
22. Leroy, J. L., Guéron, M., Mergny, J. L., and Hélène, C. (1994) *Nucleic Acids Res. 22*, 1600−1606.
23. Gallego, J., Chou, S. H., and Reid, B. R. (1997) *J. Mol. Biol. 273*, 840−856.
24. Catasti, P., Chen, X., Deaven, L. L., Moyzis, R. K., Bradbury, E. M., and Gupta, G. (1997) *J. Mol. Biol. 272*, 369−382.
25. Mergny, J. L., Lacroix, L., Han, X., Leroy, J. L., and Hélène, C. (1995) *J. Am. Chem. Soc. 117*, 8887−8898.
26. Lacroix, L., Mergny, J. L., Leroy, J. L., and Hélène, C. (1996) *Biochemistry 35*, 8715−8722.
27. Rougée, M., Faucon, B., Mergny, J. L., Barcelo, F., Giovannangéli, C., Garestier, T., and Hélène, C. (1992) *Biochemistry 31*, 9269−9278.
28. Mergny, J. L., and Lacroix, L. (1998) *Nucleic Acids Res. 26*, 4897−4903.

BI982208R